Divalent Cation Induced Fusion and Lipid Lateral Segregation in Phosphatidylcholine–Phosphatidic Acid Vesicles†

Rania Leventis,‡ Jeannine Gagné,‡ Nola Fuller,§ R. P. Rand,§ and J. R. Silvius*,‡,‖
Department of Biochemistry, McGill University, Montréal, Québec, Canada H3G 1Y6, and Division of Biological Sciences, Brock University, St. Catharines, Ontario, Canada L2S 3A1

Received February 19, 1986; Revised Manuscript Received June 5, 1986

ABSTRACT: The interactions of unilamellar vesicles containing phosphatidylcholine (PC) and phosphatidic acid (PA) in the presence of calcium and magnesium were examined by fluorometric assays of vesicle lipid mixing, contents mixing, and contents leakage and by spray-freezing freeze–fracture electron microscopy. These results were correlated with calorimetric and fluorometric measurements of divalent cation induced lateral segregation of lipids in these vesicles under comparable conditions. PA–PC vesicles in the presence of calcium show a rapid but limited intermixing of vesicle lipids and contents, the extent of which increases as the vesicle size decreases or the PA content increases. Calcium produces massive aggregation and efficient mixing of the contents of vesicles containing high proportions of dioleoyl-PA or egg PA, but vesicle coalescence in the latter case is followed rapidly by vesicle collapse and massive leakage of contents. The effects of magnesium are similar for vesicles of very high PA content. However, in the presence of magnesium, vesicles containing lower amounts of PA exhibit "hemifusion", a mode of interaction in which vesicles aggregate and mix ~50% of their lipids, apparently representing the lipids of the outer monolayer of each vesicle, without significant mixing of vesicle contents or collapse of the vesicles. Fluorometric measurements of lipid lateral segregation demonstrate that lateral redistribution of lipids in PA–PC vesicles begins at submillimolar concentrations of divalent cations and shows no abrupt change at the "threshold" divalent cation concentration, above which coalescence of vesicles is observed. By correlating calorimetric and fluorometric measurements of lipid lateral segregation and mixing of vesicle components, we can demonstrate that lipid segregation is at least strongly correlated with calcium-promoted coalescence of PA–PC vesicles and is essential to the magnesium-promoted interactions of vesicles of low PA contents.

The divalent cation mediated interactions of phospholipid vesicles have been studied extensively in recent years as a model to understand better the mechanics of the fusion process (Liao & Prestegard, 1979a; Papahadjopoulos et al., 1979; Wilschut et al., 1980, 1982; Ohki, 1984; Düzgünes et al., 1984; Rand et al., 1985). Many such studies have been carried out with vesicles containing very high proportions of anionic lipids, which coalesce rapidly and efficiently in the presence of calcium and in some cases magnesium as well. However, anionic lipids are minority components of most natural membranes, and the initial interactions between vesicles containing only these lipids are often followed rapidly by wholesale collapse of the vesicles to form dehydrated or nonlamellar phases (Papahadjopoulos et al., 1977; Portis et al., 1979; Hauser & Shipley, 1984; Miner & Prestegard, 1984; Rand et al., 1985). Accordingly, various workers have also studied the fusion of vesicles combining anionic lipids with neutral phospholipids (Liao & Prestegard, 1979a; Düzgünes et al., 1981a,b; Uster & Deamer, 1981; Sundler et al., 1981; Wilschut et al., 1982; Silvius & Gagné, 1984a,b).

Studies of interactions between membranes of heterogeneous composition encounter an inherent complication in interpretation, as different membrane components may distribute nonuniformly in the bilayer plane, creating an inhomogeneous surface whose ability to participate in membrane contact dependent processes, including fusion, varies markedly from region to region. While lateral phase separations have been demonstrated in several types of mixed-lipid systems in the presence of divalent cations and other agents (Ohnishi & Ito, 1974; Galla & Sackman, 1974; van Dijck et al., 1978; Hui et al., 1983; Graham et al., 1985), the role of lipid lateral redistributions in interactions between mixed-lipid vesicles has generally proven difficult to assess, and some results have suggested that lipid redistribution is too slow to be an important factor in lipid vesicle fusion (Hoekstra, 1982).

We have recently demonstrated that fluorescence measurements can be used to monitor reliably and specifically the lateral distribution of lipids in vesicles containing phosphatidic acid (PA)[1] and phosphatidylcholine (PC) in the presence and absence of divalent cations (Graham et al., 1985). In this study, we have correlated fluorometric observations of divalent cation induced mixing of lipids and aqueous contents (which we define operationally as "fusion") between PA–PC vesicles with direct electron microscopic observations of vesicle–vesicle

† This work was supported by the Medical Research Council of Canada (Grants ME-75800 and MA-7776), les Fonds de la recherche en santé du Québec (Grant 820040), and les Fonds pour la formation de chercheurs et l'aide à la recherche du Québec (Grant 86-EQ-2954) to J.R.S. and by the National Science and Engineering Research Council of Canada to R.P.R.

‡ McGill University.
§ Brock University.
‖ J.R.S. is the recipient of a Scholarship Award from the Medical Research Council of Canada.

[1] Abbreviations: ANTS, 8-aminonaphthalene-1,3,6-trisulfonic acid disodium salt; C_{12}-NBD-PC, 1-palmitoyl-2-[12-[(7-nitro-2,1,3-benzoxadiazol-4-yl)amino]dodecanoyl]-*sn*-glycero-3-phosphocholine; DO, dioleoyl; DPX, *p*-xylene bis(pyridinium bromide); EDTA, ethylenediaminetetraacetic acid disodium salt; egg PA, phosphatidic acid prepared from egg yolk phosphatidylcholine; egg PC, phosphatidylcholine from egg yolk; LUV, large unilamellar vesicle(s); NBD-PE, *N*-(7-nitro-2,1,3-benzoxadiazol-4-yl)phosphatidylethanolamine; PA, 1,2-diacyl-*sn*-glycero-3-phosphatidic acid; PC, 1,2-diacyl-*sn*-glycero-3-phosphocholine; PE, 1,2-diacyl-*sn*-glycero-3-phosphoethanolamine; PS, 1,2-diacyl-*sn*-glycero-3-phosphoserine; Rho-PE, *N*-(lissamine rhodamine B sulfonyl)-phosphatidylethanolamine; Tes, *N*-[tris(hydroxymethyl)methyl]-2-aminoethanesulfonic acid; EGTA, [ethylenebis(oxyethylenenitrilo)]-tetraacetic acid; DE, dielaidoyl.

0006-2960/86/0425-6978$01.50/0

interactions and with calorimetric and fluorometric measurements of PA–PC miscibility, under conditions that promote interactions between vesicles. Our results indicate that in vesicles of this type, which combine a fusion-promoting lipid (PA) with a fusion-inhibiting species (PC), lateral segregation of lipids not only accompanies vesicle fusion but, at least in some cases, is actually *required* to promote vesicle–vesicle interactions.

Materials and Methods

Materials. DOPC and egg PC were prepared as described previously (Silvius & Gagné, 1984a; Silvius et al., 1984) and converted to the corresponding PA's by hydrolysis with a crude preparation of phospholipase D from savoy cabbage, also as previously described (Graham et al., 1985). Rho-PE was synthesized from DOPE as described previously (Struck et al., 1981). NBD-PE and C_{12}-NBD-PC were obtained from Avanti Polar Lipids (Birmingham, AL). All lipids were stored as stock solutions in chloroform or hexane at −70 °C under N_2.

Ionophore A23187 was obtained from Calbiochem (La Jolla, CA), and ANTS and DPX were purchased from Molecular Probes (Junction City, OR). All common chemicals were of at least reagent grade, and all organic solvents were redistilled. Diethyl ether used in the preparation of reverse-phase evaporation vesicles was distilled from P_2O_5, then stabilized with 0.5% water, and stored at 4 °C in the dark for periods not longer than 4 weeks.

Preparation and Characterization of Vesicles. Lipid vesicles for fusion and leakage assays were prepared by reverse-phase evaporation followed by filtration through 0.1-μm Nucleopore filters, essentially as described previously (Wilschut et al., 1980). Vesicles were prepared in 200 mM NaCl, 5 mM histidine, 5 mM Tes, and 0.1 mM EDTA, pH 7.4, or in solutions of equivalent osmotic strength (determined by direct osmometry). Vesicle encapsulated volumes were determined by preparing vesicles in the presence of 5 mM carboxyfluorescein, 190 mM NaCl, 5 mM histidine, 5 mM Tes, and 0.1 mM EDTA, pH 7.4, and measuring trapped carboxyfluorescein after gel filtration as described previously (Wilschut et al., 1980). Vesicle size distributions were determined by filtration on Sephacryl S-1000 (Reynolds et al., 1983), incorporating 1 mol % NBD-PE or Rho-PE into the vesicles to allow fluorometric monitoring of the eluate.

Lipid dispersions for calorimetry were prepared by initially vortexing the lipids in 90 mM NaCl, 10 mM histidine, and 10 mM Tes, pH 7.4, above the lipid transition temperature, T_c. $MgCl_2$ was then added above T_c to a concentration of 30 mM, and the samples were then equilibrated as described previously for the preparation of PA–PC samples in the presence of calcium (Graham et al., 1985). Calorimetric thermograms were measured with a Microcal MC-1 high-sensitivity differential scanning calorimeter, as described elsewhere (Graham et al., 1985).

Lipid concentrations for both fluorometric and calorimetric samples were assayed by the procedure of Lowry and Tinsley (1974), with the modification that the digestion time was extended to 3 h.

Fusion and Leakage Assays. Mixing of vesicle lipids was assayed by the procedure of Struck et al. (1981) as modified by Hoekstra (1982). Preliminary experiments showed that the addition of calcium caused substantial and very rapid changes (up to 20%) in NBD-PE fluorescence in PA–PC vesicles containing 1 mol % each NBD-PE and Rho-PE but had little effect on the fluorescence of vesicles containing NBD-PE alone. These artifacts caused serious difficulties in the measurement of vesicle lipid mixing using the procedure of Struck et al., which measures dequenching of NBD-PE fluorescence when vesicles containing both NBD-PE and Rho-PE coalesce with unlabeled vesicles. Therefore, we assayed lipid mixing by the procedure of Hoekstra, which monitors the quenching of NBD-PE fluorescence that develops when vesicles containing 2 mol % NBD-PE coalesce with vesicles containing 2 mol % Rho-PE. To verify that the fluorescence changes registered in this assay were due to lipid probe mixing between vesicles and not simply to aggregation-induced energy transfer between probes present in the surfaces of distinct vesicles, we routinely tested the reversibility of the observed changes on addition of a twofold excess of EDTA (pretitrated with NaOH to allow for proton evolution upon binding of calcium or magnesium). Fluorescence changes induced by divalent cations were attributed to lipid mixing only when they were wholly nonreversible by a twofold excess of EDTA. Mixing of vesicle aqueous contents was assayed by the method of Ellens et al. (1985), encapsulating 50 mM ANTS in one population of vesicles and 90 mM DPX in the other. Leakage of vesicle contents was assayed by the procedure of Ellens et al. (1984), using vesicles containing both 25 mM ANTS and 50 mM DPX. In the three types of assays described above, all solutions were buffered to pH 7.4 with 5 mM histidine, 5 mM Tes, and 0.1 mM EDTA and were adjusted with NaCl to an osmolarity equivalent to that of the extravesicular medium, which contained 200 mM NaCl, 5 mM histidine, 5 mM Tes, and 0.1 mM EDTA, pH 7.4. Assays were performed at 25 °C with a vesicle lipid concentration of 30 μM except where otherwise indicated. Fluorescence values corresponding to complete intermixing of vesicle lipids or aqueous contents were calculated by using measurements from control experiments with vesicles containing 1 mol % each NBD-PE and Rho-PE or 25 mM ANTS and 45 mM DPX, respectively (Hoekstra, 1982; Ellens et al., 1985).

The divalent cation induced lateral redistribution of lipids in PA–PC vesicles was assayed fluorometrically with LUV of average diameter ~1100 Å composed of 50:45:5 DOPA/DOPC/C_{12}-NBD-PC, as described previously (Graham et al., 1985).

Rapid-Mixing, Spray-Freezing Freeze–Fracture Electron Microscopy. Suspensions of reverse-phase evaporated PA–PC vesicles, sized through 0.1-μm Nucleopore filters (~10 mM lipid after filtration), were spray-frozen without cryoprotectant after rapid mixing (~1 ms) with an equal volume of solution containing divalent cations, by using a Berger ball mixer (Rand et al., 1985). Freezing was carried out at intervals down to ~100 ms after mixing. Rapid spray-freezing, freeze-fracturing, and replicating of vesicles were done with standard procedures on Balzers 400 equipment.

Results

Factors Affecting Calcium-Induced Vesicle Interactions. In preliminary studies, we examined the calcium-mediated interactions of DOPA–DOPC vesicles under various conditions, using fluorescence assays to monitor three aspects of these interactions: lipid mixing, mixing of aqueous contents, and leakage of contents to the external medium. Representative results obtained from each type of assay are shown in Figure 1, which shows fluorescence time courses recorded after addition of 10 mM calcium to LUV (~1100-Å average diameter) composed of 50:50 DOPA–DOPC at a total lipid concentration of 30 μM. Both the mixing of vesicle contents and, more strikingly, the mixing of vesicle lipids begin at a rapid initial rate after calcium addition, but the rates of these mixing processes fall off considerably after only a short time, while the extents of mixing are still far from complete. The

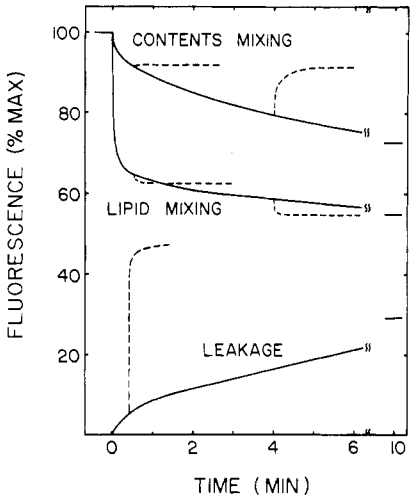

FIGURE 1: Time courses of fluorescence changes observed in the contents-mixing, lipid-mixing and leakage assays when 50:50 DOPA–DOPC vesicles (average diameter ~1100 Å) are exposed to 10 mM $CaCl_2$ at $t = 0$. Dashed curves show the effects of EDTA addition at the indicated times on the fluorescence signal.

fluorescence changes observed in the lipid-mixing assay are entirely stable upon addition of excess EDTA (Figure 1, dashed line). When the free calcium concentration is subsequently returned to 10 mM, no further rapid lipid mixing is observed (not shown). The calcium-induced mixing of vesicle contents is also almost entirely fixed when excess EDTA is added during the rapid initial phase of mixing, but EDTA at longer times (~1 min) substantially reverses the fluorescence changes developed through contents mixing. Interestingly, the leakage assay shows a rapid and substantial release of vesicle contents when excess EDTA is added even at very short times (~5 s) after calcium addition.

The origin of the rapid but incomplete intermixing of DOPA–DOPC vesicle components in the presence of calcium was investigated further, by using the lipid-mixing assay to examine the coalescence of vesicles of different average sizes. When LUV prepared by filtration through 0.1-μm pore-size Nucleopore membranes are bath-sonicated for increasing periods of time, the average vesicle diameter gradually decreases, as can be demonstrated by both encapsulated volume measurements and gel filtration on Sephacryl S-1000 (not shown). Figure 2A shows time courses of lipid mixing induced by calcium between 30:70 DOPA–DOPC vesicles (initial diameter ~1100 Å) that were bath-sonicated for increasing lengths of time. Smaller vesicles clearly show more extensive lipid mixing when calcium is added. To verify that this effect is truly attributable to variations in the vesicle size and not in the vesicle concentration (which increases as the mean vesicle size decreases), we also examined the dependence of the lipid-mixing kinetics on the vesicle concentration. In Figure 2B are shown time courses of lipid mixing obtained with various concentrations of 50:50 DOPA/DOPC vesicles of diameter ~1100 Å. When these time courses are replotted as a function of X_0t, where X_0 is the initial concentration of vesicles (or of lipid) and t is the time after calcium addition, the traces become superimposable from 0.6 μM up to at least 60 μM lipid, as expected for a second-order process of constant maximal amplitude (Bentz et al., 1983; Ellens et al., 1984). The extent of rapid lipid mixing induced by calcium between DOPA–DOPC vesicles thus is independent of the vesicle concentration but varies inversely with the vesicle size.

The results presented above appear to leave only two plausible explanations for the "self-limiting" nature of the

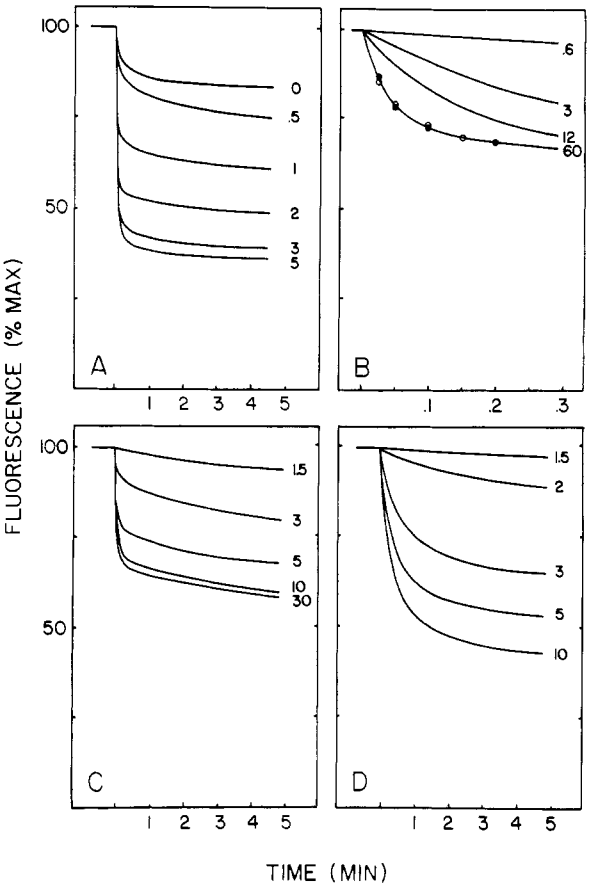

FIGURE 2: Time courses of lipid probe mixing upon addition of divalent cations to DOPA/DOPC vesicles. (A) Effect of vesicle size. $CaCl_2$ (10 mM) was added at $t = 0$ to 30:70 DOPA–DOPC vesicles (initial diameter ~1100 Å) that were bath-sonicated for the indicated number of minutes to reduce their mean diameter. The average vesicle diameter (estimated from trapped-volume measurements) gradually falls from ~1100 Å with no sonication to ~250 Å after 5 min of sonication. (B) Effect of vesicle concentration. $CaCl_2$ (10 mM) was added at $t = 0$ to 50:50 DOPA/DOPC vesicles (~1100-Å diameter) at varying lipid concentrations (0.6–60 μM, as indicated). Open and filled circles represent data for 0.6 and 3.0 μM lipid, respectively, plotted to the same X_0t scale as for 60 μM lipid (see text). (C and D) Effect of divalent cation concentration. At $t = 0$ either (C) $CaCl_2$ or (D) $MgCl_2$ was added to 50:50 DOPA/DOPC vesicles (average diameter ~1100 Å) to give the indicated divalent cation concentrations (in millimolar).

calcium-promoted intermixing of PA–PC vesicle components. First, the vesicles may be able to fuse, or even to undergo significant lipid mixing, only until they grow to exceed some critical size. Second, vesicles may be able to fuse only so long as they maintain a transmembrane gradient of calcium that is rapidly collapsed through vesicle–vesicle interactions (Liao & Prestegard, 1979b). The importance of vesicle size in determining the extent of calcium-induced lipid mixing has been demonstrated above. To evaluate the possible importance of an asymmetric transmembrane gradient of calcium in promoting vesicle fusion, we examined the effect of the calcium ionophore A23187 on lipid mixing between 50:50 DOPA–DOPC vesicles (~1100-Å diameter). A modest and variable inhibition of calcium-induced lipid mixing, ranging from ~40% to almost 0 in different experiments, could be demonstrated only at high levels of the ionophore (~1:50 or 1:25 mol/mol of lipid). Significantly, these relatively weak inhibitory effects of the ionophore were not enhanced when the vesicle concentration was lowered from 30 to 3 μM to slow the rate of vesicle aggregation. Incorporation of buffers including 50 mM EDTA or EGTA into 50:50 or 30:70

DOPA–DOPC vesicles failed to enhance the extent of calcium-induced lipid mixing over that observed with similar vesicles prepared without internal chelators. Therefore, the role of a transmembrane calcium gradient in promoting the vesicle interactions that lead to lipid mixing appears uncertain.

Effects of Vesicle Composition and Divalent Cation Levels. The experiments described above, which examined the effects of vesicle size, concentration, and transmembrane calcium asymmetry on lipid mixing between vesicles, were carried out with a fixed calcium concentration (10 mM) and a constant vesicle composition (50:50 or, in a few experiments, 30:70 DOPA–DOPC). In this section, we describe the effects of the vesicle composition and the divalent cation concentration on vesicle–vesicle interactions. Except where otherwise noted, these experiments were carried out with ~1100-Å diameter vesicles at a lipid concentration of 30 μM.

Parts C and D of Figure 2 show fluorescence time courses observed with the lipid-mixing assay when calcium or magnesium chloride at various levels was added to 50:50 DOPA–DOPC vesicles. Both divalent cations produce a rapid but partial lipid mixing at all concentrations above a characteristic "threshold" level. The fluorescence changes induced by either cation were completely preserved on addition of excess EDTA. As the initial phase of the lipid mixing is quite rapid for vesicles of widely varying PA contents, we chose to quantitate the divalent cation induced lipid mixing by measuring the fluorescence quenching developed at a fixed time (90 s) after divalent cation addition. This sampling time allowed the rapid phase of lipid mixing to proceed nearly to completion but avoided artifacts that arose from the flocculation of vesicles containing high levels of PA at long times.

In Figure 3A,B, the extent of rapid lipid mixing is plotted as a function of the calcium or magnesium concentration for vesicles containing various proportions of DOPA and DOPC. The extent of lipid mixing increases with the divalent cation level above the threshold concentration but plateaus at high levels of calcium or magnesium. Plots of initial lipid mixing rates vs. the divalent cation concentration gave quite similar behavior (not shown). As the vesicle PA content rises, the threshold concentration of divalent cations needed to initiate lipid mixing decreases, while the extent of lipid mixing at high levels of divalent cations increases. Control measurements of vesicle trapped volumes and size distributions (see Materials and Methods) showed that these differences between vesicles of varying PA content are not attributable to differences in vesicle size (data not shown). Magnesium is only slightly less effective than calcium in promoting lipid mixing at low divalent cation concentrations and actually produces more lipid mixing at high concentrations than does calcium.

To evaluate to what extent the results just presented are influenced by vesicle size, we repeated some of the experiments just presented using vesicles of different sizes (average diameter ~260–300 Å or ~1200 Å), giving the results summarized in Figure 3C,D. At fixed vesicle PA content, a reduction in vesicle size invariably reduces the threshold calcium level needed to induce lipid mixing. At high calcium levels, the extent of rapid lipid mixing reaches a plateau level, which is almost independent of size for vesicles containing ≥50% PA but which is inversely dependent on size for vesicles containing lower amounts of PA. For vesicles of any fixed size, an increase of PA content lowers the calcium threshold and increases the extent of rapid lipid mixing at high calcium levels, as was observed above for ~1100-Å vesicles.

The results shown in Figure 4 illustrate the effects of divalent cations on the mixing and leakage of the aqueous

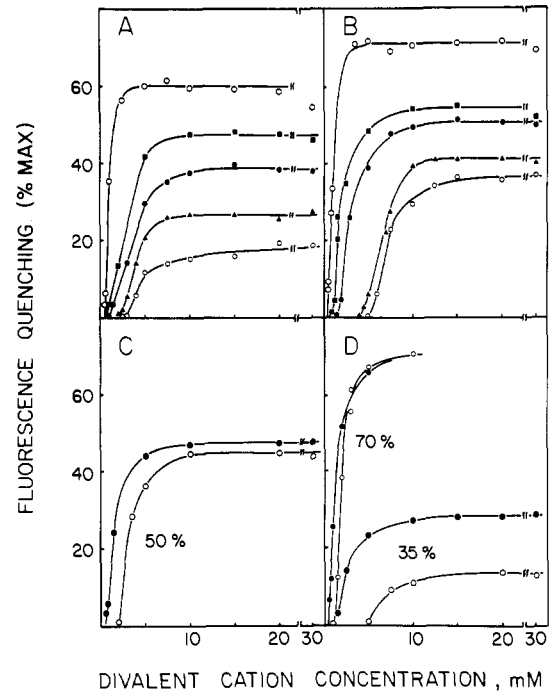

FIGURE 3: Extent of rapid lipid probe mixing (after 90 s) when DOPA–DOPC vesicles of different PA contents were exposed to calcium or magnesium. (A and B) ~1100-Å vesicles containing (○) 80%, (■) 60%, (●) 50%, (▲) 40%, or (◦) 35% DOPA were mixed with either (A) calcium or (B) magnesium at varying concentrations. (C) DOPA/DOPC vesicles (50:50) were prepared with an average diameter of ~1200 Å (open circles) by filtration through 0.2 μM membranes or with an average diameter of ~260 Å (filled circles) by filtration and bath sonication for 180 s. Lipid mixing was initiated by addition of varying concentrations of calcium. (D) The experiments in (C) were repeated with vesicles containing either 70 or 35 mol % DOPA, as indicated.

contents of PA–PC vesicles of different compositions. Calcium produces a rapid but limited mixing of the contents of 50:50 DOPA–DOPC vesicles, as well as a slow leakage of contents. Magnesium produces almost no intermixing of the contents of these vesicles and a negligible rate of leakage (Figure 4A,B). Vesicles containing 80% DOPA exhibit more extensive mixing of contents (Figure 4C) but similarly low leakage rates (Figure 4D) in the presence of either calcium or magnesium. The kinetics of contents mixing and leakage were second order in the vesicle concentration up to at least 50 μM lipid in the presence of 10 mM $CaCl_2$ or $MgCl_2$, but the reaction order decreased slightly at higher lipid concentrations when contents mixing was induced by magnesium ions. Plots of the initial rates of vesicle contents mixing as a function of the divalent cation concentration (not shown) are very similar in form to the plots of lipid mixing vs. divalent cation concentration shown in Figure 3. The threshold concentrations of calcium or magnesium required to elicit significant mixing of vesicle components, and the plateau region in which the initial rate of mixing becomes independent of the divalent cation concentration, are the same whether these parameters are determined by either the lipid-mixing or the contents-mixing assay. However, as the results obtained with magnesium for 50:50 DOPA–DOPC vesicles most clearly indicate, the extent of lipid mixing is not always directly correlated with the extent of contents mixing, and this discrepancy cannot be attributed simply to the leakage of vesicle contents.

As noted above, the rapid fluorescence changes observed in the contents-mixing assay are almost entirely fixed by addition of excess EDTA at short times after divalent cation addition. However, addition of EDTA at longer times (several

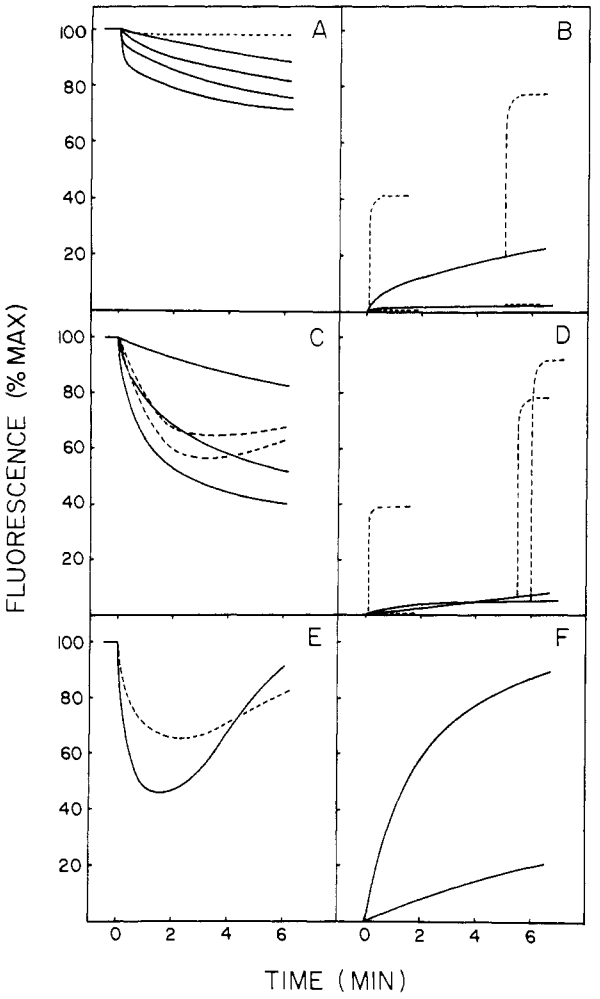

FIGURE 4: Contents mixing and leakage during fusion of PA–PC vesicles. (A) Contents mixing induced between 50:50 DOPA–DOPC vesicles by 30 mM $MgCl_2$ (dashed curve) or 2, 5, 10, and 30 mM $CaCl_2$ (solid curves, top to bottom). (B) Leakage of contents from 50:50 DOPA–DOPC vesicles induced by 10 mM $CaCl_2$ (upper solid curve) or $MgCl_2$ (lower solid curve). Dashed lines show the effects of addition of a twofold excess of EDTA at the indicated times. (C) Contents mixing induced between 80:20 DOPA–DOPC vesicles by 2, 5, and 10 mM $CaCl_2$ (solid curves, top to bottom) or 5 and 10 mM $MgCl_2$ (upper and lower dashed curves). (D) Leakage of contents from 80:20 DOPA–DOPC vesicles induced by 10 mM $CaCl_2$ (initially higher solid curve) or 10 mM $MgCl_2$ (initially lower solid curve). Dashed lines show the effects of addition of a twofold excess of EDTA. (E) Mixing of contents between 80:20 egg PA–egg PC vesicles induced by 10 mM $CaCl_2$ (solid curve) or $MgCl_2$ (dashed curve). (F) Leakage of contents from 80:20 egg PA–egg PC vesicles induced by 10 mM $CaCl_2$ or $MgCl_2$ (upper and lower curves, respectively).

minutes) largely reverses these fluorescence changes. The fluorescence quenching produced by contents mixing becomes susceptible to reversal by EDTA more rapidly when calcium rather than magnesium is used to trigger vesicle coalescence. Parallel measurements of vesicle leakiness show that divalent cations alone cause relatively slow leakage, but subsequent addition of excess EDTA induces considerable release of vesicle contents (Figures 4B,D). Interestingly, when vesicles are treated successively with calcium and excess EDTA, the extent of release of vesicle contents by EDTA (as measured by the leakage assay) can be much greater than the extent of mixing of vesicle contents at the moment of EDTA addition (as measured by the contents-mixing assay). This is particularly true when the vesicles contain lower proportions of PA (~ 50%) or when EDTA is added at very short times after calcium addition (~1 s). In contrast, previous studies of other vesicle systems that fuse in the presence of divalent cations (Wilschut et al., 1980, 1982, 1983; Sundler & Papahadjopoulos, 1981) have usually reported that addition of excess EDTA at early times after divalent cation addition, when contents mixing is still well short of maximal, causes relatively little release of vesicle contents. However, these conclusions often appear to be based chiefly on results obtained with contents-mixing assays, where addition of EDTA shortly after addition of divalent cations largely fixes the fluorescence changes developed due to contents mixing at that point. Our present results demonstrate that contents-mixing and leakage assays can in some cases give rather different pictures of the stabilities of vesicles under such conditions (see, for example, Figure 1). This result is different from that obtained by Wilschut et al. (1980) in a study of the calcium-mediated fusion of phosphatidylserine vesicles, where contents-mixing and contents-leakage assays yielded comparable estimates of the extent of release of vesicle contents that is triggered by addition of EDTA at various times after calcium addition.

To evaluate how changes in the lipid acyl chain composition can influence the stability and the coalescence of PA-containing vesicles in the presence of divalent cations, we also examined the behavior of vesicles prepared from mixtures of egg PA and egg PC. Vesicles prepared from 100% egg PA or from 80:20 or 50:50 egg PA/egg PC behaved very much like DOPA–DOPC vesicles of equal PA content in the lipid-mixing assay (results not shown). As well, calcium- or magnesium-induced mixing of vesicle contents is only moderately faster for egg PA–egg PC vesicles than for DOPA–DOPC vesicles (Figure 4E). However, at 25 °C, vesicles containing egg PA show enormously faster rates of contents leakage in the presence of calcium or magnesium than do vesicles containing DOPA (Figure 4F). At 37 °C, the rate of calcium-induced contents leakage from egg PA vesicles was ~30% lower than that observed at 25 °C, while vesicles of DOPA showed a slight increase in the leakage rate on raising the temperature from 25 to 37 °C. However, calcium-induced contents leakage was still much faster for egg PA-containing than for DOPA-containing liposomes even at the higher temperature.

Electron Microscopic Studies. To visualize more directly the nature of the divalent cation promoted interactions between PA–PC vesicles, we examined suspensions of these vesicles by freeze–fracture electron microscopy after rapid mixing with divalent cations and spray-freezing as described by Rand et al. (1985). In Figure 5A is shown a representative micrograph of 50:50 DOPA/DOPC vesicles in the absence of divalent cations. It is evident that the vesicles show some variability in diameter, although the average vesicle diameter estimated from the micrographs is consistent with the value estimated from trapped-volume measurements (~1100 Å). One preparation of 50:50 DOPA/DOPC vesicles also contained, in addition to vesicles of the size shown in Figure 5A, a small population of very large vesicles (diameters up to ~8000 Å) with smaller vesicles trapped inside. The 80:20 PA/PC vesicles gave a size distribution quite similar to that observed for 50:50 PA/PC vesicles, in agreement with results from our trapped-volume and gel filtration experiments.

The addition of calcium (10 mM) to dispersions of 50:50 DOPA/DOPC vesicles leads to modest but clearly visible changes in the vesicle size distribution, as shown in Figure 5B for a suspension of vesicles (lipid concentration ~5 mM) that was treated with calcium for ~1 min prior to spray-freezing. After calcium treatment, the average vesicle size is significantly increased, in part because the smallest of the vesicles existing before calcium treatment seems to have largely disappeared.

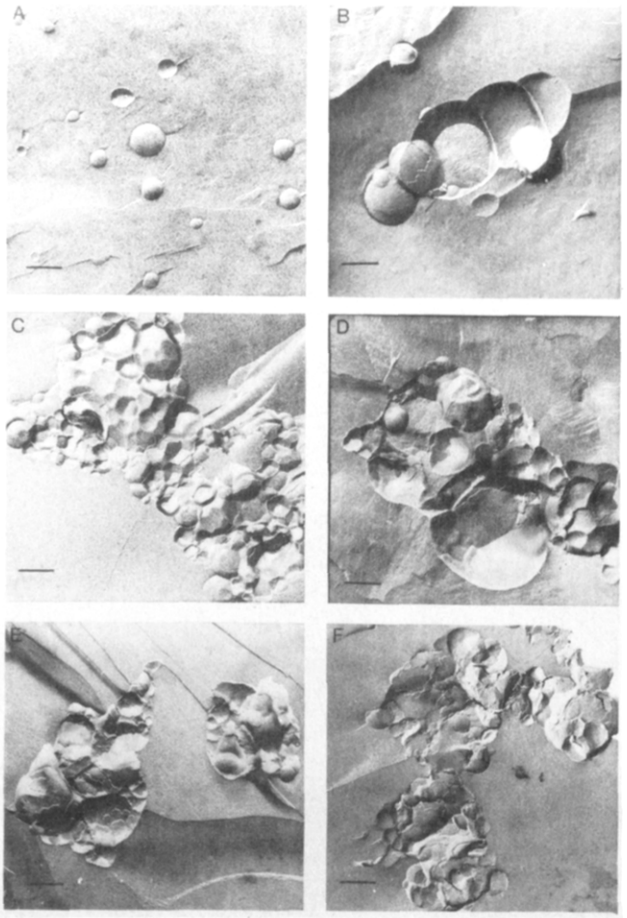

FIGURE 5: Freeze–fracture electron micrographs (space bar = 0.2 μm) of PA–PC dispersions that were rapidly mixed with divalent cations ($CaCl_2$ or $MgCl_2$ to 10 mM) and spray-frozen after a specified time. (A) Vesicles containing 50:50 DOPA–DOPC, before calcium addition. (B) DOPA–DOPC vesicles (50:50) ~1 min after addition of $CaCl_2$. (C) DOPA–DOPC vesicles (50:50) ~1 min after addition of $MgCl_2$. (D) DOPA–DOPC vesicles (80:20) ~1 min after addition of $CaCl_2$. (E) Egg PA–egg PC vesicles (80:20) ~100 ms after addition of $CaCl_2$. (F) Same as (E) ~1 min after addition of $CaCl_2$.

Aggregates of vesicles can be observed, and many bilamellar diaphragms can be observed in these aggregates in regions of extensive intervesicle contact, as Rand et al. (1985) have reported previously for phosphatidylserine vesicles treated with calcium. However, the average number of vesicles in these aggregates is small, and isolated vesicles, or aggregates of only two or three vesicles, are quite commonly observed.

A dispersion of 50:50 DOPA/DOPC vesicles that was treated with 10 mM magnesium showed a quite different microscopic appearance, as the micrograph shown in Figure 5C illustrates. Magnesium causes a much more extensive aggregation of these vesicles than does calcium. However, while extensive vesicle–vesicle contacts can be seen in the magnesium-induced aggregates, there is little indication of significant breakdown in the integrity of the vesicle membranes, which would lead to vesicle fusion or collapse. Reinforcing this conclusion, we note that the size distribution of individual vesicles, which are readily discernible within these aggregates, is not noticeably different from the distribution of vesicle sizes before treatment with magnesium. The magnesium-induced aggregates of these vesicles appeared very similar at ~100 ms and ~1 min after magnesium addition. It thus appears that magnesium can cause extensive aggregation and surface apposition of 50:50 DOPA/DOPC vesicles but causes little if any intercommunication of the interior spaces of these vesicles. By contrast, calcium induces less extensive aggregation of these vesicles, but it can induce a limited but significant coalescence of the interior compartments of the vesicles, particularly those with smaller diameters.

The micrograph shown in Figure 5D demonstrates the effects of calcium on a dispersion of 80:20 DOPA/DOPC vesicles. After ~1 min exposure to calcium, these vesicles are more extensively aggregated than are vesicles containing equimolar DOPA and DOPC under the same conditions (Figure 5B). Micrographs of 80:20 DOPA/DOPC vesicles quenched at very short times after calcium addition (~100 ms) showed aggregates that resembled those shown in Figure 5D but were on average slightly smaller (not shown). While some of the vesicles shown in Figure 5D, particularly those on the edges of the aggregates, remain intact, it appears that appreciable coalescence of vesicles has taken place in the centers of the aggregates.

The initial behavior of 80:20 egg PA/egg PC vesicles after addition of calcium is similar to that of 80:20 DOPA/DOPC vesicles, but the behavior of the two preparations differs at longer times. Dispersions of the egg PA/egg PC vesicles that are frozen at very short times after calcium addition have formed aggregates very similar to those formed by 80:20 DOPA/DOPC vesicles (Figure 5E). However, after ~1 min in the presence of calcium, the egg PA/egg PC vesicle aggregates show flattened surfaces and complex fracture planes that suggest that the interior spaces of the aggregates have largely collapsed at this time (Figure 5F). By contrast, aggregates of 80:20 (or 50:50) DOPA/DOPC vesicles still appear to retain substantial interior aqueous volumes after ~1–2-min exposure to calcium (Figure 5B,D).

The concentration of lipid in the electron microscopic samples (~5 mM) was about 100-fold greater than that used in the fluorescence experiments described above. Therefore, to the extent that the early events observed by freeze-fracturing are rate-limited by vesicle aggregation, a second-order process, we expect that freeze-fracture images obtained for samples frozen within ~100 ms of divalent cation addition will represent events taking place within the first several seconds after divalent cation addition in the fluorescence assays. Later events (i.e., further transformations observed by electron microscopy in vesicle aggregates ~1–2 min after divalent cation addition) are less likely to be strictly aggregation limited. Therefore, freeze–fracture images obtained at longer times (~1 min) probably represent events occurring over a time scale of a few minutes after divalent cation addition in the fluorescence experiments.

Relationship of Fusion to PA–PC Phase Separation. Phosphatidylcholine is usually considered to exert an inhibitory effect on the aggregation and fusion of lipid vesicles (Düzgünes et al., 1981a,b; Sundler et al., 1981; Silvius & Gagné, 1984b). As small PA–PC vesicles containing even relatively high proportions of PC can still exhibit significant (albeit limited) mixing of lipid and/or contents in the presence of calcium or magnesium (this work; Liao & Prestegard, 1979a, 1981), we investigated the possibility that such fusion requires the lateral segregation of PA-enriched domains in the vesicle membranes. In a previous study (Graham et al., 1985), we demonstrated that phase separation occurs at high calcium concentrations in vesicles containing ≥10 mol % PA in PC, with kinetics comparable to or faster than the rates observed for vesicle lipid and contents mixing in the experiments presented above. These results are consistent with the possibility that lateral segregation of PA may play an important role in the divalent cation induced interactions of PA–PC vesicles. In this study, we further tested this possibility by examining the correlation

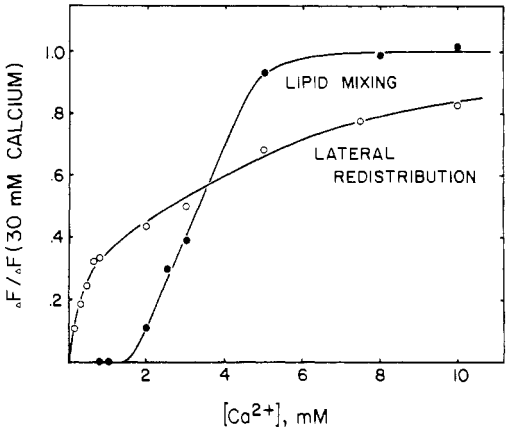

FIGURE 6: Lipid lateral redistribution (monitored by self-quenching of the fluorescence of C_{12}-NBD-PC) and fusion [monitored by the procedure of Hoekstra (1982)], for ~50:50 DOPA–DOPC vesicles as a function of the calcium concentration. Fluorescence changes in the two types of assays are plotted as fractions of the fluorescence change observed at 30 mM $CaCl_2$, in order to facilitate comparison of the concentration dependence.

between vesicle–vesicle interactions and lateral segregation of PA when vesicles are treated with low levels of calcium or with magnesium.

We have shown previously that lipid lateral redistributions in DOPA–DOPC vesicles can be monitored through changes in the fluorescence of vesicle-incorporated C_{12}-NBD-PA or -PC. If PA–PC vesicles containing one of these probes are exposed to conditions that promote demixing of PA and PC, the probe molecules themselves will redistribute in the bilayer plane, and an increased self-quenching of fluorescence results when, and only when, the probe concentration in the bilayer exceeds a few mole percent (Graham et al., 1985). The data presented in Figure 6 show how the self-quenching of fluorescence in 50:45:5 DOPA/DOPC/C_{12}-NBD-PC vesicles varies with the calcium concentration in the medium. For comparison, the extent of rapid lipid mixing between 50:50 DOPA/DOPC vesicles is also shown as a function of the calcium concentration. It is evident that a substantial lateral redistribution of lipid begins at calcium concentrations well below the threshold for (aggregation-limited) lipid mixing (1.5 mM) and shows no abrupt change at the threshold. The interaction of PA–PC vesicles in the presence of calcium is thus invariably correlated with a rapid lateral redistribution of lipids, regardless of the calcium concentration. To examine further the generality of this correlation, we also examined the effects of magnesium on the lateral distribution of lipids in PA–PC bilayers under conditions that promote vesicle–vesicle interactions.

As a necessary first step, we used calorimetry to determine phase diagrams for two PA–PC mixtures in the presence of magnesium, which have not previously been reported. Representative thermograms for mixtures of DEPC and DEPA in the presence of high magnesium levels are shown in Figure 7A. The thermograms are qualitatively very similar to those observed previously for this lipid system in the presence of high levels of calcium (Graham et al., 1985), and they can be analyzed in an entirely similar way to give the phase diagram shown in Figure 7B. For the purposes of the present discussion, the most important feature of this phase diagram is the left-hand vertical boundary of the two-phase region existing between 22 and 94 °C, since this boundary defines the bilayer concentration of DEPA below which no phase separation will occur in the presence of magnesium. By observing the presence or absence and the amplitude of the endotherm at 22 °C in

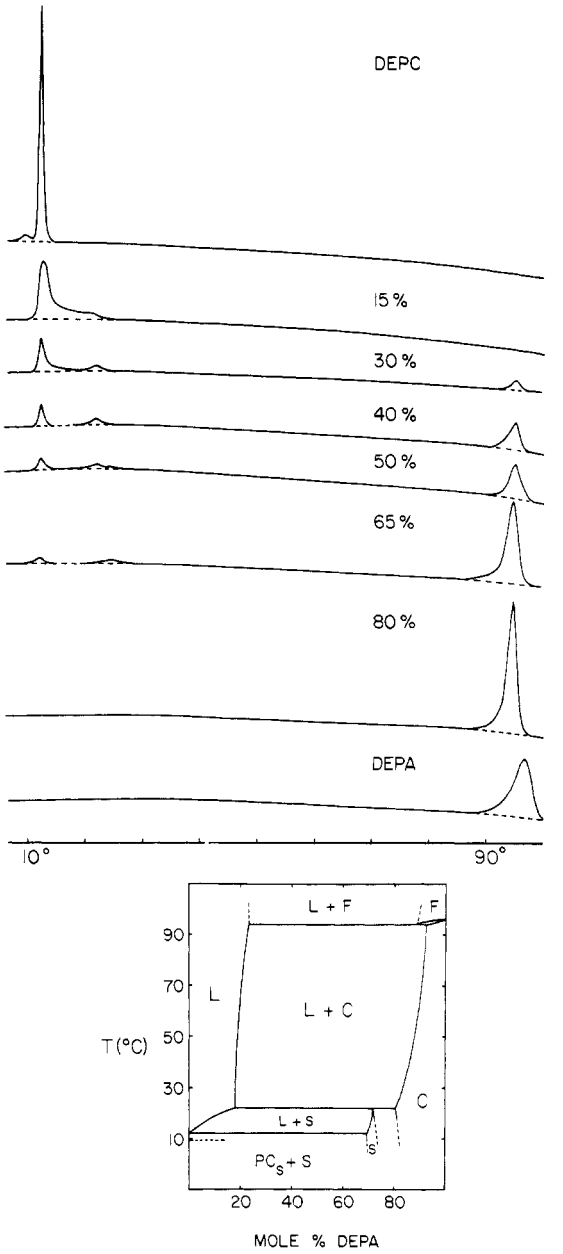

FIGURE 7: (A) Calorimetric thermograms measured for DEPA–DEPC samples of the indicated PA contents in the presence of 30 mM $MgCl_2$. Details of sample preparation are described under Materials and Methods. (B) Phase diagram for the DEPA–DEPC (Mg^{2+}) system, derived from the calorimetric data shown in (A). The following symbols are used to designate different phases: L, lamellar liquid crystalline; C, cochleate phase rich in DEPA (Mg^{2+}); PC_S, solid phase of nearly pure DEPC; S, solid solution of DEPC and DEPA (Mg^{2+}); F, high-temperature fluid phase of DEPA (Mg^{2+}).

thermograms of different DEPA–DEPC mixtures, we can determine that the 22 °C three-phase line begins at ~15 mol % DEPA. The enthalpy of the 94 °C endotherm in these same samples extrapolates to 0 at ~23 mol % DEPA, indicating that the three-phase line at 94 °C begins at this molar proportion of DEPA. The left-hand boundary of the region of phase separation between 22 and 94 °C therefore gradually shifts from ~15 mol % DEPA at the lower temperature to ~23 mol % DEPA at the higher temperature. The calorimetrically determined phase diagram for the DMPA–DMPC (Mg^{2+}) system (not shown) indicates quantitatively comparable miscibility of these two species in the presence of magnesium. While we cannot determine directly the phase diagram for the DOPA–DOPC (Mg^{2+}) system by calorimetry,

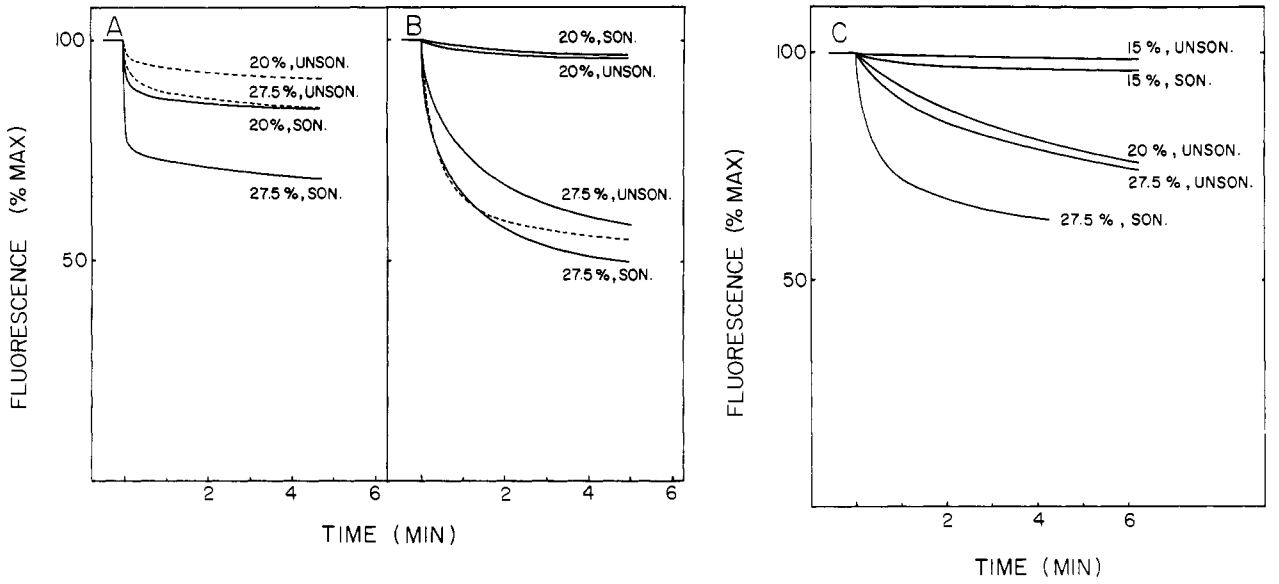

FIGURE 8: (A and B) Time courses of lipid mixing observed when (A) 30 mM $CaCl_2$ or (B) 30 mM $MgCl_2$ is added to vesicles containing 20 or 27.5 mol % DOPA in DOPC. Traces labeled "UNSON" were obtained with vesicles of average diameter ~1100 Å, while traces labeled "SON" were obtained with vesicles bath-sonicated for 180 s, to a final average diameter of ~260 Å. The dashed curve in (B) shows the time course for ~1100-Å vesicles containing 27.5 mol % DOPA, replotted to a 4 times slower time base. (C) Time courses of lipid mixing observed when 30 mM $MgCl_2$ is added to vesicles containing 15, 20, or 27.5 mol % DEPA in DEPC, as indicated, at 42 °C. Traces obtained with unsonicated vesicles (~1100-Å diameter) and vesicles bath-sonicated for 180 s are indicated as in (A) and (B). The time course obtained on a fourfold slower time base for unsonicated vesicles containing 27.5 mol % DEPA (not shown) was similar in rate and shape to the trace shown for sonicated vesicles with this PA content.

it appears reasonable to conclude that the solubility of DOPA in liquid-crystalline DOPC in the presence of magnesium is similar to that for the other PA–PC mixtures, i.e., ~20 mol %. By contrast, PA–PC mixtures in the presence of calcium phase-separate when the bilayers contain as little as 10 mol % PA (Graham et al., 1985).

Fluorescence experiments using DOPA/DOPC/C_{12}-NBD-PC vesicles (not shown) demonstrated that the magnesium-induced lateral redistribution of lipids in these vesicles exhibits rapid kinetics (≤1 s) and is significant even at submillimolar concentrations of magnesium, similar to the results obtained previously with calcium (Graham et al., 1985). However, magnesium-induced demixing of PA and PC, as monitored by C_{12}-NBD-PC fluorescence measurements, was somewhat less extensive than that induced by calcium, in agreement with the calorimetric results described above.

Parts A and B of Figure 8 show the effects of calcium and magnesium on the mixing of lipids between 27.5:72.5 and 20:80 DOPA/DOPC vesicles with average diameters of ~1100 or ~260 Å (estimated from trapped-volume measurements). Calcium addition to vesicles of either composition produces a rapid but very limited mixing of lipids, the extent of which increases as the average vesicle diameter decreases. The addition of magnesium to 27.5:72.5 DOPA–DOPC vesicles produces a considerably greater extent of lipid mixing, which approaches ~50% at long times. When these vesicles are bath-sonicated for 180 s, reducing the average vesicle diameter to ~260 Å, the extent of lipid mixing induced by magnesium is nearly unchanged, although the rate of mixing is considerably increased. In dramatic contrast to these results, the addition of magnesium to 20:80 DOPA–DOPC vesicles produces no significant mixing of lipids, regardless of the average vesicle diameter. To examine the generality of this result, we also measured the magnesium-induced mixing of lipids between DEPA–DEPC vesicles with low PA contents. As the traces shown in Figure 8C demonstrate, DEPA–DEPC vesicles behave in a qualitatively similar fashion to DOPA–DOPC vesicles in the presence of magnesium. For the dielaidoyl lipid vesicles, however, the threshold level of PA, below which magnesium-induced lipid mixing falls off to negligible levels, appears to lie near ~15 mol % PA vs. ~20 mol % PA for DOPA–DOPC vesicles.

Discussion

While several previous studies have examined various aspects of the interactions of PA–PC vesicles (Lansman & Haynes, 1975; Koter et al., 1978; Liao & Prestegard, 1979a,b, 1980; Sundler et al., 1981), these studies have varied widely in the sizes and compositions of the vesicles examined, experimental parameters such as temperature and pH, and the techniques used to examine vesicle–vesicle interactions. In this study, we have combined several experimental approaches in an attempt to provide a reasonably complete picture of the overall processes of vesicle interactions and lipid redistribution mediated by divalent cations in a two-component model membrane system.

One of the most singular features of the divalent cation induced fusion of PA–PC vesicles is that the extent of fusion depends markedly on the vesicle size, even when the vesicles are much larger than the small unilamellar vesicles (SUV) for which the effects of vesicle radius on fusion ability have been demonstrated most dramatically (Liao & Prestegard, 1979a). Vesicles containing higher levels of PA show more extensive intermixing of lipids and aqueous contents than do vesicles of comparable initial size but lower PA content. A similar conclusion was reported previously by Liao and Prestegard (1979a), who examined the fusion of concentrated suspensions of SUV with low PA contents. By using larger vesicles, we can now show that this relationship extends even to high vesicle PA contents and very high ratios of divalent cations to phospholipids.

While calcium and magnesium behave similarly in promoting the fusion of vesicles that contain high amounts of PA (80–100 mol %), the two divalent cations differ markedly in their effects on vesicles containing smaller amounts of PA (≤50 mol %). For vesicles composed of 50 mol % each DOPA and

DOPC, calcium promotes a rapid but only partial mixing of both lipids and aqueous contents. By contrast, magnesium produces virtually no leakage or mixing of the contents of these vesicles, yet this species produces considerable lipid mixing. Our electron microscopic results with these vesicles (Figure 5C) support these observations, showing that magnesium promotes extensive aggregation and apposition of vesicle surfaces but no apparent vesicle collapse or coalescence of the vesicles' interior compartments. A similar phenomenon has been observed by Ellens et al. (1985) in a study of the magnesium-mediated interactions of vesicles composed of PE and cholesterol hemisuccinate. This behavior appears to reflect a mode of vesicle interaction that may be termed "hemifusion", in which the vesicles establish direct surface contacts, allowing efficient exchange of lipids between the outer monolayers of different vesicles, without proceeding to actual fusion events in which the vesicles' inner monolayers and aqueous contents would also coalesce. It is interesting that magnesium-promoted hemifusion of vesicles containing $\leq$50% PA can actually produce more lipid mixing than the calcium-promoted fusion of the same vesicles, which is strongly sensitive to the vesicle size. In a situation such as this, the lipid-mixing assay not only may overestimate the rate of vesicle fusion under a particular set of conditions but may also lead to erroneous conclusions regarding the relative rates of fusion of vesicles under two or more apparently similar sets of conditions. From an examination of all our results from lipid- and contents-mixing assays, it appears that hemifusion is at most a minor factor in the calcium-promoted mixing of lipids between PA–PC vesicles. By contrast, this process represents virtually the exclusive mechanism for magnesium-induced lipid mixing between vesicles containing $\leq$50 mol % PA and may well be a significant feature in the initial stages of magnesium-promoted interactions between vesicles of higher PA content.

The results of freeze–fracture electron microscopy help to explain and to extend the results obtained from fluorescence assays of PA–PC vesicle lipid and contents mixing and leakage in the presence of divalent cations. Vesicles that are very rich in PA rapidly form large aggregates after addition of divalent cations. This finding might suggest that the very substantial mixing of vesicle contents that is observed fluorometrically after divalent cation addition takes place in the formation of large aggregates rather than through interactions between pairs of individual vesicles. However, the kinetics of contents mixing between these vesicles in the presence of calcium or magnesium are second-order in the vesicle concentration, at least up to $\sim$50 μM lipid. Therefore, in this range of vesicle concentrations, the rate of contents mixing is limited by the rate of aggregation of vesicles (Bentz et al., 1983). Efficient mixing of contents thus can occur even within a simple interacting pair of vesicles. The subsequent growth of large vesicle aggregates leads to collapse of vesicles containing high amounts of egg PA, as Rand et al. (1985) have observed previously when PS vesicles are treated with calcium. These workers have pointed out that the membranes of aggregated vesicles experience considerable lateral stress as vesicle–vesicle adhesion causes deformation of the vesicles from a spherical shape. The rapid collapse of egg PA-rich vesicles after aggregation may reflect vesicle rupture brought about by such lateral stress. However, vesicles rich in DOPA rapidly form very similar large aggregates and exhibit similar rates of contents mixing in the presence of divalent cations, yet the rate of contents leakage and collapse for these vesicles under such conditions is much less than for vesicles containing egg PA. This observation of a differential effect of PA acyl chain composition on vesicle contents mixing vs. vesicle collapse suggests that the two processes are, to a considerable extent, dissociable for the vesicle fusion events examined here. By appropriate choices of lipid acyl chain compositions, it may be possible to modify differentially the tendencies of other lipid vesicle systems to exhibit "productive" fusion leading to contents mixing, as opposed to leakage and collapse under a given set of conditions.

In previous studies of the calcium-induced interactions of vesicles containing phosphatidylcholine and anionic lipids (Silvius & Gagné, 1984b; Graham et al., 1985), we have suggested that these interactions are correlated with lateral segregation of PC-depleted regions in the vesicle surface, through which intervesicle contact actually takes place. The findings of this paper support this suggestion, and they provide particularly strong evidence that lateral separation of PA-enriched domains is essential for the magnesium-promoted hemifusion of vesicles containing $\leq$50 mol % PA in PC.

As reported previously (Liao & Prestegard, 1979a), small vesicles containing even low molar proportions of PA and PC can exhibit calcium-promoted fusion. By contrast, even small unilamellar vesicles ($\sim$250 Å) composed of PS and PC are unable to fuse in the presence of calcium when the vesicles contain less than $\sim$50 mol % PS (Düzgünes et al., 1981a). We suggest that this qualitative difference between PA–PC and PS–PC vesicles arises largely from the fact that PA can segregate laterally from PC in the presence of calcium even when the vesicles contain as little as $\sim$10 mol % PA (Graham et al., 1985) while PS–PC vesicles show such phase separation only when the PS content is much higher ($\geq$40 mol %; Silvius & Gagné, 1984b). The results in this paper, and those of Graham et al. (1985), demonstrate that lateral segregation of PA in PA–PC vesicles is rapid enough, and occurs at low enough divalent cation concentrations, to play a significant role in the calcium- or magnesium-promoted interactions of these vesicles. More convincing evidence that lateral segregation of PA plays an obligatory role in these interactions would be provided by a demonstration that such interactions abruptly cease when the PA content is lowered to the point where no phase separation can take place. This result is difficult to establish unequivocally for the case of calcium-promoted fusion, as the threshold level of PA, below which no phase separation occurs in the presence of calcium, is very low ($\leq$10%). In this range of vesicle PA contents, the vesicle size becomes a major factor in determining the extent of vesicle fusion, and it could be argued that the fusion of vesicles of very low PA content is limited less by the PA content than by the limit to which their size can be reduced by even prolonged sonication (Liao & Prestegard, 1979a). However, magnesium-induced hemifusion between PA–PC vesicles is less sensitive in extent, if not in rate, to the vesicle size, and relatively rapid fluorescence changes, corresponding to mixing of $\sim$50% of the vesicle lipids, can be observed by the lipid-mixing assay when magnesium is added to vesicles containing as little as 27.5 mol % DOPA or DEPA. It is therefore striking to find that vesicles containing 20 mol % DOPA or 15 mol % DEPA exhibit negligible lipid mixing, even at high magnesium levels and after extensive sonication. This result can be correlated with our calorimetric results, which indicate that PA–PC mixtures do not phase separate at higher temperatures in the presence of magnesium until the bilayer PA content exceeds $\sim$15–20 mol %. It appears, therefore, that hemifusion between PA–PC vesicles in the presence of magnesium requires at least a limited lateral segregation of PA-enriched domains.

Previous studies of calcium-induced lipid phase separations and fusion of PS–PC vesicles (Hoekstra, 1982) have concluded

that the fusion process is much faster than lateral redistributions of lipids in this system. This result would appear to indicate that lateral segregation of PS-enriched domains plays no role in the fusion of these vesicles, in contrast to our conclusions for the PA–PC vesicle system. However, we believe that the apparent differences in the behavior of the PS–PC and PA–PC systems may in fact reflect differences in the behavior of the fluorescent probes that were used to monitor lipid lateral distributions in the two systems, as discussed previously (Silvius & Gagné, 1984b; Graham et al., 1985). Further study will be needed to clarify this point. In any event, it is clear that for PA–PC vesicles it is possible for one bilayer to interact directly with another through laterally segregated domains of composition different from that of the bilayer as a whole, even when the average composition of the bilayer is unsuitable to support such interactions. This result underscores that to understand how the various lipid (and other) components of membranes can participate in the process of membrane fusion, it can be important to address the question of how these species are laterally distributed in the membrane bilayer.

ACKNOWLEDGMENTS

We thank Dr. Martin Zuckerman and Dr. Joe Bentz for useful and stimulating discussions during the course of this work.

Registry No. DOPA, 61617-08-1; DOPC, 4235-95-4; Ca, 7440-70-2; Mg, 7439-95-4.

REFERENCES

Bentz, J., Nir, S., & Wilschut, J. (1983) *Colloids Surf. 6*, 33–66.

Düzgünes, N., Nir, S., Wilschut, J., Bentz, J., Newton, C., Portis, A., & Papahadjopoulos, D. (1981a) *J. Membr. Biol. 59*, 115–125.

Düzgünes, N., Wilschut, J., Fraley, R., & Papahadjopoulos, D. (1981b) *Biochim. Biophys. Acta 642*, 182–195.

Düzgünes, N., Paiement, J., Freeman, K. B., Lopez, N. G., Wilschut, J., & Papahadjopoulos, D. (1984) *Biochemistry 23*, 3486–3494.

Ellens, H., Bentz, J., & Szoka, F. (1984) *Biochemistry 23*, 1532–1538.

Ellens, H., Bentz, J., & Szoka, F. (1985) *Biochemistry 24*, 3099–3106.

Galla, H. J., & Sackmann, E. (1974) *Biochim. Biophys. Acta 399*, 103–115.

Graham, I., Gagné, J., & Silvius, J. R. (1985) *Biochemistry 24*, 7123–7131.

Hauser, H., & Shipley, G. G. (1984) *Biochemistry 23*, 34–41.

Hoekstra, D. (1982) *Biochemistry 21*, 2833–2840.

Hui, S. W., Boni, L. T., Stewart, T. P., & Isac, T. (1983) *Biochemistry 22*, 3511–3516.

Koter, M., de Kruijff, B., & van Deenen, L. L. M. (1978) *Biochim. Biophys. Acta 514*, 255–263.

Lansman, J., & Haynes, D. M. (1975) *Biochim. Biophys. Acta 394*, 335–347.

Liao, M.-J., & Prestegard, J. H. (1979a) *Biochim. Biophys. Acta 550*, 157–173.

Liao, M.-J., & Prestegard, J. H. (1979b) *Biochem. Biophys. Res. Commun. 90*, 1274–1279.

Liao, M.-J., & Prestegard, J. H. (1981) *Biochim. Biophys. Acta 601*, 453–461.

Lowry, R. I., & Tinsley, I. J. (1974) *Lipids 9*, 491–493.

Miner, V. W., & Prestegard, J. H. (1984) *Biochim. Biophys. Acta 774*, 227–236.

Ohki, S. (1984) *J. Membr. Biol. 77*, 265–275.

Ohnishi, S., & Ito, T. (1974) *Biochemistry 13*, 881–887.

Papahadjopoulos, D., Vail, W. J., Newton, C., Nir, S., Jacobson, K., Poste, G., & Lazo, R. (1977) *Biochim. Biophys. Acta 465*, 579–598.

Paphadjopoulos, D., Poste, G., & Vail, W. L. (1979) *Methods Membr. Biol. 10*, 1–121.

Portis, A., Newton, C., Pangborn, W., & Papahadjopoulos, D. (1979) *Biochemistry 18*, 780–790.

Rand, R. P., Kachar, B., & Reese, T. S. (1985) *Biophys. J. 47*, 483–490.

Reynolds, J. A., Nozaki, Y., & Tanford, C. (1983) *Anal. Biochem. 130*, 471–474.

Silvius, J. R. (1982) in *Lipid-Protein Interactions* (Jost, P. C., & Griffith, O. H., Eds.) Vol. 2, pp 239–281, Wiley-Interscience, New York.

Silvius, J. R., & Gagné, J. (1984a) *Biochemistry 23*, 3232–3240.

Silvius, J. R., & Gagné, J. (1984b) *Biochemistry 23*, 3241–3247.

Silvius, J. R., McMillen, D. A., Saley, N. D., Jost, P. C., & Griffith, O. H. (1984) *Biochemistry 23*, 538–547.

Struck, D. K., Hoekstra, D., & Pagano, R. E. (1981) *Biochemistry 20*, 4093–4099.

Sundler, R., & Papahadjopoulos, D. (1981) *Biochim. Biophys. Acta 649*, 743–750.

Sundler, R., Düzgünes, N., & Papahadjopoulos, D. (1981) *Biochim. Biophys. Acta 649*, 751–758.

Uster, P. S., & Deamer, D. W. (1981) *Arch. Biochem. Biophys. 209*, 385–395.

van Dijck, P. W. M., de Kruijff, B., Verkleij, A. J., van Deenen, L. L. M., & de Gier, J. (1978) *Biochim. Biophys. Acta 512*, 84–96.

Wilschut, J., Düzgünes, N., Fraley, R., & Papahadjopoulos, D. (1980) *Biochemistry 19*, 6011–6021.

Wilschut, J., Holsappel, M., & Jansen, R. (1982) *Biochim. Biophys. Acta 690*, 297–301.

Wilschut, J., Düzgünes, N., Hong, K., Hoekstra, D., & Papahadjopoulos, D. (1983) *Biochim. Biophys. Acta 734*, 309–318.